

Properties of Pure and distorted Nickel Sulfide Ni_{1-x}S and NiS_{1-x}

Chhama Pandey^a, Gulzar Ahmed^a, C.Kumar Dixit^c, Yamini Sharma^b

^aDept. of Physics, Mewar University, Chittorgarh-312901

^bTheoretical Condensed Matter Physics Laboratory, Dept. of Physics, Feroze Gandhi College, Raebareli-229001

^cDepartment, of Physics Dr. Shakuntala Misra National Rehabilitation University Lucknow U.P. India-226017

Corresponding Author: Chhama Pandey, Department of Physics, Mewar University, Chittorgarh-312901, Email: tiwari.chhama1990@gmail.com

ABSTRACT

The dimorphic behaviour of Nickel monosulfide consists high temperature hexagonal phase and low temperature rhombohedral phase. We focused our study for the high temperature hexagonal phase of NiS. On the creation of defect in NiS the space group is changed from $P6_3/mmc$ to $P-3m1$ and $P-6m2$ for Ni^+S and NiS^+ respectively. Ni-S bond length is 2.35 Å which is in very good agreement with experimental Ni-S bond length of 2.39 Å^[7]. We also studied the effect of potentials on the band structure of NiS and found that number of states of Fermi level marginally decreases for positive potential gradient and increases for negative potential gradient maintaining its metallic nature. Partial density of states confirmed that near Fermi level Ni-d states and S-p states affect all optical, electronic as well as thermal properties. Here we compared both hexagonal and millerite phases of NiS and found that both phases are nearly similar. In the context of optical properties we found that we can enhance or reduce the intensities of transitions in different regions. The order of resistivity for different stoichiometry of NiS are $\text{Ni}_{1-x}\text{S} > \text{NiS}_{1-x} > \text{NiS}$ and for effect of different potentials gradient the order of resistivity are $\text{NiS}_{3\text{eV}} > \text{NiS}_{1.5\text{eV}} > \text{NiS} > \text{NiS}_{-1.5\text{eV}} > \text{NiS}_{-3\text{eV}}$.

Keywords: Nickel Sulfides; electronic band structure; Optical and transport properties

1. Introduction:

Transition metals such as Fe, Co and Ni form several isotropic series of sulphide structures which include monosulphides with the NiAs structures and disulphide with pyrite structure. The general characteristics of the two phases of monosulphides of Ni i.e. high temperature NiAs type and low temperature millerite (hexagonal) have been fabricated and presented in great details by number of researchers. Rajamani and Prewit discussed the dimorphic behavior of NiS i.e. high temperature hexagonal phase and low temperature millerite NiS, which is the rhombohedral [1]. The calorimetric investigation for insulator to metal (IM) transition in Ni_{1-x}S was reported by Polovov et al. They concluded that the acoustic lattice vibrations dominated the process of stabilization of NiS [2]. Hexagonal nickel sulfide exhibits metal-non metal transitions accompanied by changes in magnetic, electrical and structural properties at Neel temperature ($T_N=265^\circ\text{K}$) [3]. Controversy for the ground state behaviour of hexagonal NiS was resolved by Sharma et al. They confirmed the occurrence of first order phase transition in NiS [4]. The electronic structure of millerite phase of NiS was thoroughly studied using electron spectroscopic measurements by Krishna Kumar et al. A comparative study between hexagonal and millerite phase of NiS provided information about difference in covalency [5]. Different properties of NiS such as electrical, optical and structural properties were reported by Atay et al. They also concluded that NiS exhibits interesting metal insulator phase transition showing antiferromagnetic semiconducting and paramagnetic properties at low and high temperature [6]. X-ray diffraction study for millerite phase of NiS was performed and

calculated under different pressure condition [7]. The structural, electronic and vibrational properties of various phases of nickel sulfides i.e. NiS, Ni₃S₂, NiS₂ and Ni₃S₄ were studied by ab-initio method. The Ni-S bonds have found to be highly covalent. The down shifting of the d-band centers of nickel sulfides made sulfur contaminated Ni electrode less active toward hydrogen fuel oxidation [8]. The phase transition of defect hexagonal nickel sulfide was studied by positron annihilation spectroscopy. Fan et al. concluded that the transition temperature decreases and thermal hysteresis width narrows down with deficient Ni contents in Ni_{1-x}S [9]. Nickel sulfide thin films with different sulphur content were prepared and their structural, physical and optical properties were studied. From the XRD spectra it was observed that the optical band gap and activation energy were strongly dependent on Ni/S ratio [10]. Electronic and spectral properties of hexagonal NiS have been studied at high as well as low temperature using (LDA+DMFT) DFT theory and showed the importance of electron correlation effects for proper understanding of optical properties [11]. Boughalmi et al. investigated NiS for their optical properties through transmittance and reflectance spectra [12], a low optical band gap was obtained from the absorption spectra.

The review of the above materials explains different electronic, optical as well as thermal properties of temperature dependent phases but there is a lack of a systematic study. In our work we have studied bulk nickel sulfide, nickel and sulfur deficient NiS. We also studied the effect of electric field on bulk NiS. We also studied the physical properties of NiS and also compare the effects of different exchange correlation potentials.

1.2. Computational Methodology:

We have adopted the full potential linearized augmented plane wave's method [FP-LAPW] which is based on the density functional theory (DFT) and is one of the most accurate band structure methods. It is used to calculate the electronic, optical properties from the fully converged results. The GGA developed by Wu and Cohen was used. The convergence of this basis set is controlled by a cut-off parameter $R_{MT}K_{max}=7$, where K_{max} is the magnitude of the largest k-vectors. The maximum radial expansion l_{max} is set to be 10. The iteration is halted when the difference charge density and energy was less than $0.0001 e^- a_0^{-3}$ and 0.001 Ry respectively between steps taken as convergence criterion. The energy cut-off between the core and valence states was set at -6.0 Ry. The R_{MT} for Ni and S are 2.44 and 1.99 Å respectively and for millerite NiS [12] are 2.49 and 2.55 for Ni and S respectively .

1.3. Results and discussion:

1.3.1 Structural Properties:

NiS has the dimorphic behaviour [1-7] i.e. a high temperature hexagonal phase and a low temperature rhombohedral phase which is also known as millerite NiS. Millerite NiS follows pyramidal geometry i.e. Ni atom has five nearest S atoms while in the hexagonal phase Ni atom has four nearest S atom. In this work, we study the high temperature phase i.e. hexagonal NiS which has the NiAs structure with P63/mmc space group. Lattice parameters for NiS are $a=3.4395\text{Å}$, $c=5.3514\text{Å}$ [7]. We first optimized these experimental parameters for our system to obtain the lowest energy. The optimized lattice parameters are $a=3.434\text{ Å}$, $c=5.1003\text{ Å}$. We see that experimental c/a ratio is 1.55[7] where as calculated c/a is 1.48. The Wyckoff position of Ni is 2a i.e. (0, 0, 0) and S possess 2(c) i.e. (1/3, 2/3, 1/4). The crystal structure and optimization curve of NiS are shown in fig. 1(a) and 1(b).

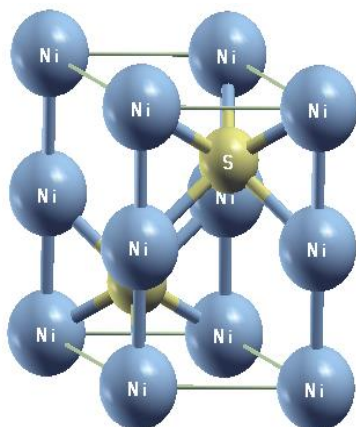


Fig. 1(a): Structure of hexagonal NiS

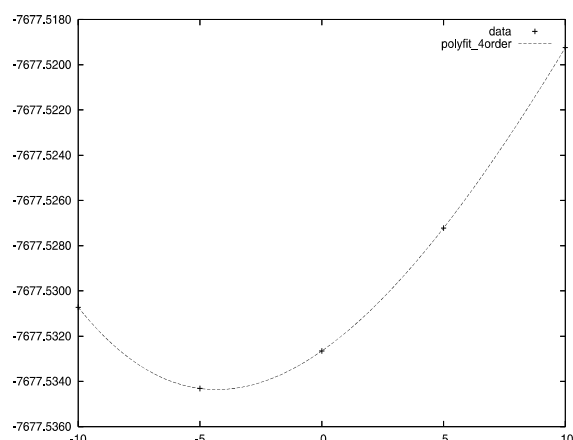


Fig. 1 (b): Optimization curve for hexagonal NiS

When Ni-atom and S-atom are removed from NiS, the space group for non-stoichiometric NiS is changed from space group 194 to 164 for Ni⁺S and 187 for NiS⁺, maintaining its hexagonal structure. The shifts of Fermi energy levels of Ni⁺S and NiS⁺ from NiS are 0.3696, 0.3362 and 0.6335 eV respectively. The convergence energy, bond length etc are also mentioned in the given table [1]. We observe that Ni-S bond length increased for Ni deficient NiS where as S-S bond length increases for S deficient NiS.

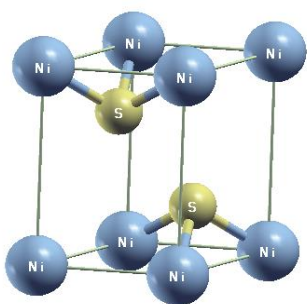


Fig. 1.2(a) Structure of Ni⁺S

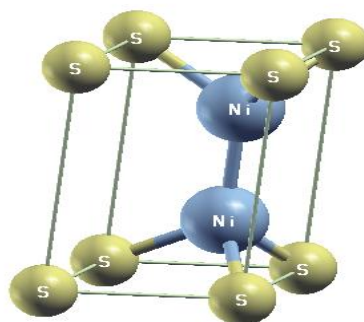
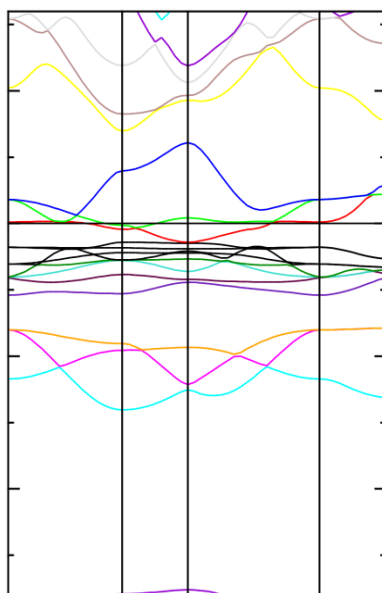


Fig. 1.2(b) Structure of NiS⁺

The Ni-S bond length 2.35Å is in good agreement with experimental Ni-S bond length of 2.39 Å [7]. Shorter or longer bond length indicates strong/weak hybridization on creation of defects in NiS. Convergence energies, charges, bond lengths, R_{MT} of NiS, Ni⁺S and NiS⁺ are tabulated in Table 1.

1.3.3 Electronic Properties:

The density of states and energy band structure give information about materials and also useful to explain many properties such as the optical spectra and transport properties of solids. In order to explain the contribution from different atomic orbital, we have calculated the total and partial density of states (DOS). In Fig. 1.3 (a) we have plotted energy band diagram as well as density of states in Fig. 1.3



(b) of NiS and deficient NiS⁺ and Ni⁺S. The Fermi level (E_F) is set at 0 eV and coincides with the top of the valence band. In the energy band diagrams we can see that at Fermi level E_F , bands cross over which explain the metallic nature of NiS. The energy bands are plotted along high symmetry direction Γ -M-K- Γ -A in the energy range from -14.0 to 8 eV. The bands from -14.0 to 0 eV correspond to valence bands (VB) while bands from 0 to 8 eV lie in the conduction bands (CB). Shift of bands can be easily explained from density of states. From DOS of NiS, Ni⁺S and NiS⁺, we see that no. of states /eV per unit cell at the Fermi level varies. In NiS, 1.84 states reduced to 1.36 states /eV and increases to 4.23 states /eV for Ni⁺S and NiS⁺ respectively. From this variation of number of states at Fermi level, we may conclude that number of the states at Fermi level decreases for Ni deficient NiS and increases for S deficient NiS. From the partial density of states of NiS we see that from energy range -8.0 to 1.66 eV, Ni states mainly contributes, in which a peak occur at -2.06 eV in valence band, contributed by Ni-d states. Near Fermi level Ni-d states mainly contributes from -5.64 eV to 1.57 eV and Ni d sharp peak occurs of 4.34 states /eV. Sulphur states occurs from -8.05 eV to 11.86 eV in which sulfur-s states do not contribute much whereas Sulfur-p states contributes from -8.16 eV to 3.39 eV and -2.18 to 1.68 eV. We have perturbed the structure of NiS by de-intercalation of one Ni-atom and one S-atom. As we see from the total dos of NiS, at Fermi level Ni-d states and Sulfur-p states mainly contribute. We observed from that partial dos of Ni-d states that in Ni⁺S states no. of states are decreasing and Ni-d states are smeared in valence band while S-p states are narrowed towards conduction bands. From sulphur deficient NiS, number of states of Ni- d states at Fermi level increases, Ni-d states are narrowed toward conduction band S states at Fermi level as well as in valence band are smeared.

An overall contribution of states is observed for deficient NiS, although metallic nature is maintained. The number of states at E_F are changed which will modify the optical and transport parameters. Greater presence of Ni-d states and Sulfur-p in NiS⁺ shows that deficiency of sulphur atoms modifies the electronic structure of NiS to a greater extent.

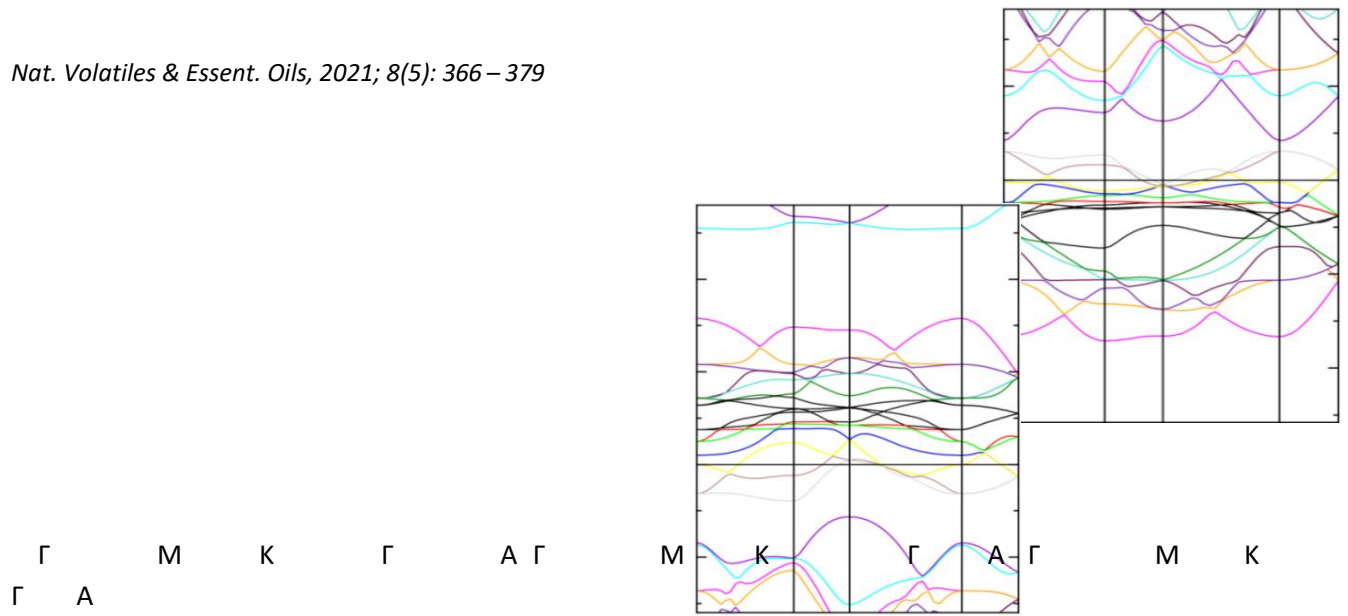


Fig. 1.3(a): Energy band Diagram of NiS, Ni²S and Ni³S₂

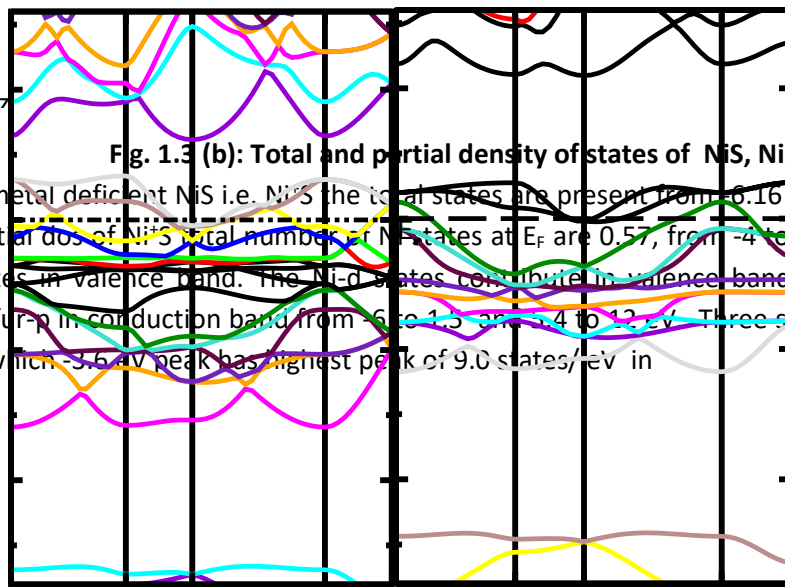


Fig. 1.3 (b): Total and partial density of states of NiS, Ni²S and Ni³S₂

In metal deficient NiS i.e. Ni²S the total states are present from -6.16 to 1.5 eV and 5.39 to 12 eV. From partial dos of Ni²S total number of Ni states at E_F are 0.57, from -4 to 3.00 eV there is large peaks of Ni states in valence band. The Ni-d states contribute in valence band and with small contribution Ni, Sulfur-p in conduction band from -6 to 1.5 eV and 4 to 12 eV. Three sharp peak at -1.6, -3.6 and -5.0 eV in which -3.6 eV peak has highest peak of 9.0 states/eV in

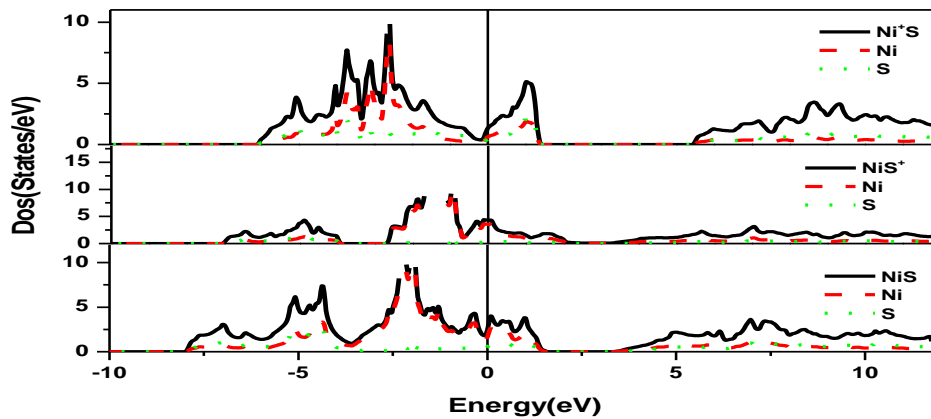
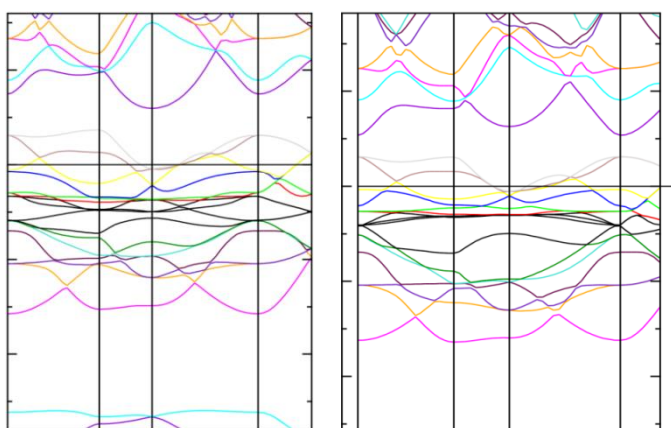


Fig 1.4 (a): Energy bands of on NiS : applied electric fields **Fig 1.4 (b): Energy bands of on NiS : applied of positive and negative 1.5 V/Å** **electric fields positive and negative 3.0 V/Å**



valence band while only one sharp peak occurs at 1.1 eV of S-p states of 1.07 states/eV in conduction band . We also wish to study the effect of applied electric fields on the band structure of NiS. The energy band diagram and the density of states are shown in Fig. 1.4 (a) and Fig. 1.4 (b) respectively.

From the plot of density of states, we see that on the application of positive and negative electric field of 1.5 V/Å. The number of states at E_F are 1.89, 1.49, 2.23 for NiS, NiS_{-1.5}, NiS_{1.5} respectively while on the application of 3V/Å potential difference the no. of states at E_F are 1.47 and 2.67 respectively i.e. the no. of states at the Fermi level marginal decreases for positive potential gradient and increases for negative electric field while maintaining the metallic nature.

From the partial dos, we see that the first peak for NiS which occur at -0.30 of 4.1 states and second peak -1.88 eV of 9.37 states shifts towards valence band i.e. -0.43eV with 3.45 states and -2.17eV with 9.3 states for -1.5 electric field. The first peak occurs at 0.21eV and second peak of -1.5 eV of 0.47 states on the application of positive 1.5 V/Å. We may conclude that on application of negative electric fields, Ni

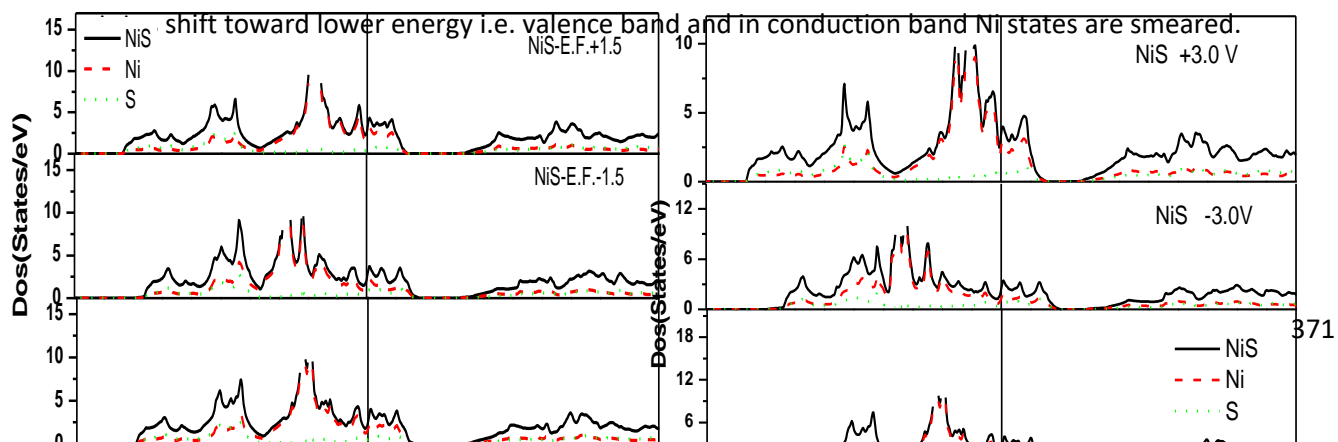
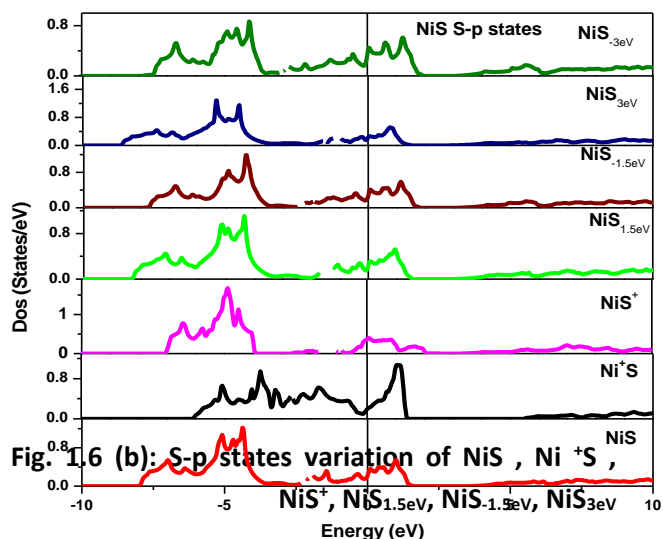
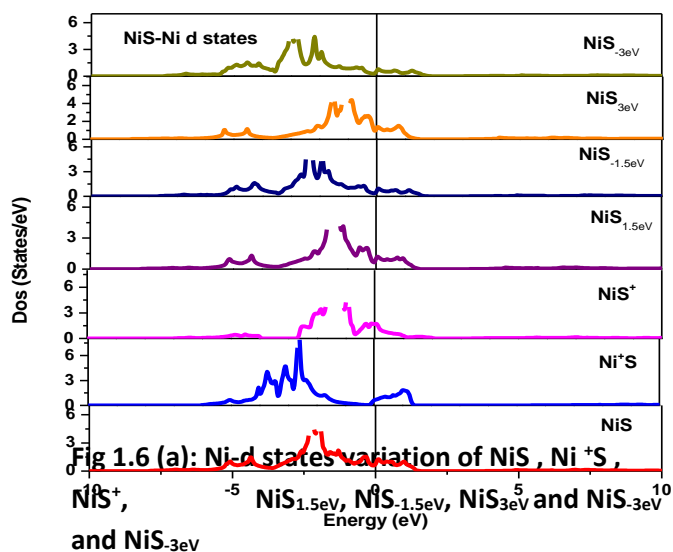


Fig. 1.5: Density of states of NiS, positive and negative electric fields of 1.5 and 3V/Å

In presence of +1.5 V/Å electric field we see that states of Ni are shifting towards higher energies i.e. two peak of NiS at -0.30, -1.88 eV shifts to -0.21, -1.57eV. The S-states are not affected by the potential gradient. In the conduction band, states from 0 to 1.55 eV contract to 1.4 eV which are Ni and S hybridized states.

We have made a comparative study for NiS, disordered NiS and also studied the effect of varying electric field on NiS. From partial density of states (PDOS) we confirm that near E_f , Ni-d states and S-p states contribute which affects all properties by these states.



On deintercalation of Ni atom ($Ni_{1-x}S$), Ni-d states decrease and S-p states increase whereas on the removal of S atom (NiS_{1-x}), contribution of both Ni-d and S-p states increase. On application of external electric field, Ni-d states decreases whereas presence of S-p states increases. Further in case of Ni deficiency in NiS, Ni-d states shift towards lower energies whereas in NiS^+ , sulfur states shift toward higher energies. On application of positive potential peaks of Ni-d and S-p states shift toward higher energies whereas on application of negative potential, Ni-d states shift toward lower energies and S-p states shift towards higher energies.

On comparing energy bands as well as dos of hexagonal NiS with millerite NiS [12], we see that behavior of both phases are quite similar although there is all shift of states towards Fermi level. We also observe that near Fermi level there is strong hybridization of Ni-d and S-p states. From anti bonding states in the

hexagonal system similar to millerite NiS phase. Charge transfer energy is smaller in the millerite phase compared to hexagonal.

The above variations are responsible for different optical as well as transport properties which are sensitive to the states in the vicinity of Fermi level.

1.3.3. Optical Properties:

Optical properties can be explained in the term of complex frequency dependent dielectric functions, which are divided into two parts. The imaginary part which depends on interband and intraband transitions as well as on the momentum matrix which is calculated by considering all the possible transitions from occupied to unoccupied states. The real and imaginary parts of dielectric function completely explain the optical properties of materials at all photon energies. We have calculated the energy dependent electron energy loss spectra (EELS) for our selected compounds which are a very important tool for explaining interband transitions in valence band. Scattering probabilities of volume losses is directly related to energy loss function. Starting of loss function is associated with the transition of electrons from top of the valence bands to bottom of the conduction bands. We have calculated optical properties in both xx and zz- directions due to hexagonal structure of NiS shown in Fig 1.7. In xx direction near IR region it is increasing and near 4500 nm, a sharp peak is observed in bulk NiS. On application of positive potential of 1.5 and 3V/Å, the NiS peak shifted to near IR region. Variation in the eloss are related to the shifting of bands. As we can see that in Ni⁺S there is shifting of bands towards valance band i.e. lower energy and in NiS⁺ bands are shifting towards conduction band i.e. higher energies.

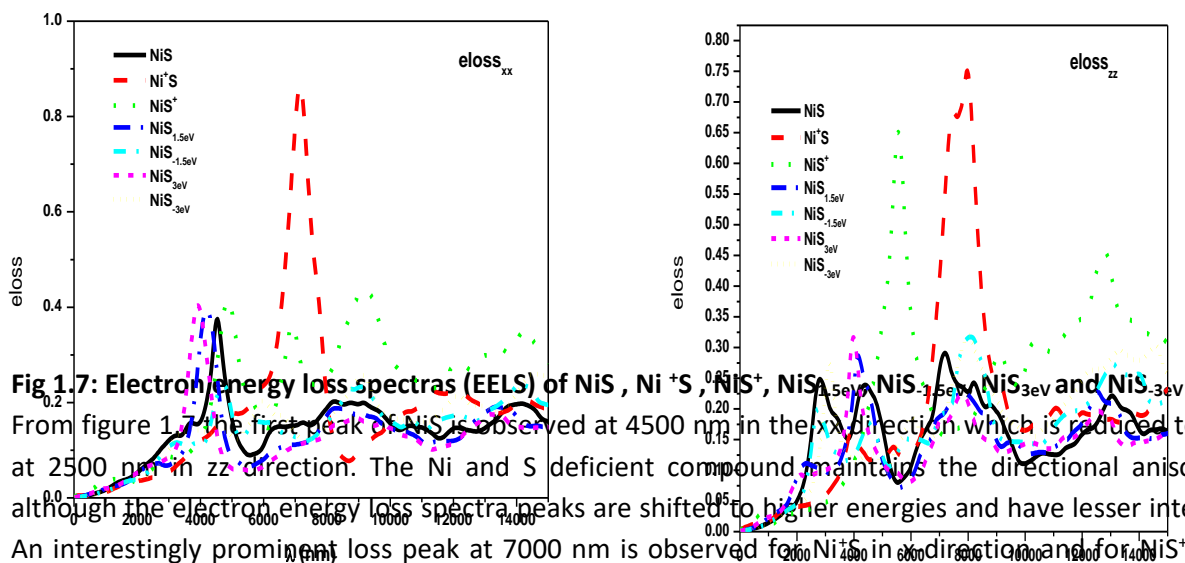


Fig 1.7: Electron energy loss spectra (EELS) of NiS, Ni⁺S, NiS⁺, NiS^{-1.5eV}, NiS^{-1.5eV}, NiS^{-3eV} and NiS^{-3eV}
 From figure 1.7 the first peak of NiS is observed at 4500 nm in the xx direction which is reduced to 0.24 at 2500 nm in zz direction. The Ni and S deficient compound maintains the directional anisotropy although the electron energy loss spectra peaks are shifted to higher energies and have lesser intensity. An interestingly prominent loss peak at 7000 nm is observed for Ni⁺S in z-direction and for NiS⁺ in z-direction. The vacancies created due to deficiency of Ni or S lead to the observed losses in the spectra. Application of positive or negative electric field allows the loss spectra to a great extent in IR or visible region but effects the loss spectra in uv and lower uv regions due to gain in energy by charge carriers. In zz direction the EELS of NiS is 0.24 at 2800 nm wavelength and on applying positive as well as negative potential there is shift in IR region.

Absorption is a reverse process to photoluminescence i.e. the creation of electron-hole pair when photon is absorbed by a compound, undergoes recombination and emits a photon with random phase,

polarization and direction. From the absorption peak in the absorption spectra we get the information

Parameters/Properties	NiS	Ni ²⁺ S	Ni ³⁺ S
-----------------------	-----	--------------------	--------------------

about photoluminescence.

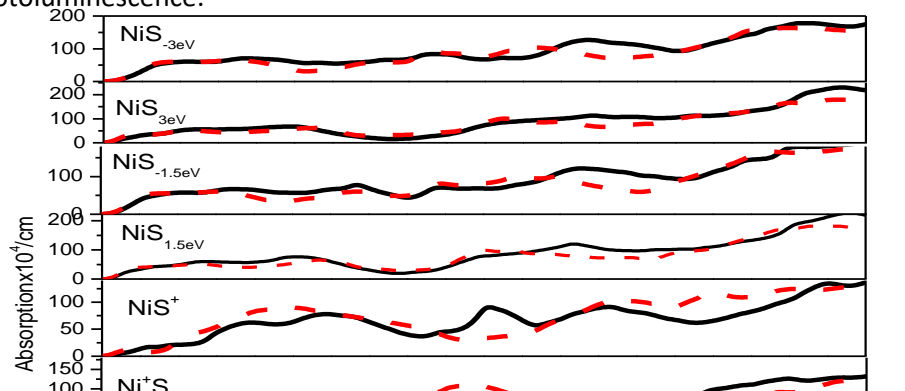


Fig. 1.8: Absorption coefficient of NiS, Ni²⁺S, Ni³⁺S, NiS₃, NiS₃, NiS₃ and NiS₃

The metallic behavior of NiS is confirmed from the spectra since the absorbance peak starts from 0.1 eV. In NiS³ transition starts from 0 eV (optical band gap is present) with lower absorption peak in IR region i.e. at 1 eV ($21 \times 10^4/cm$). In the visible region between 1.7 to 3.3 eV, it increases upto $75 \times 10^4/cm$. On the application of electric field to NiS, intensity of peaks in the absorption spectra are marginally reduced.

Table 1.1: Structural and input parameter

Space Group and Lattice parameter (Å)	194 a=3.434 c=5.1003	164 a=3.4347 c=5.1003	187 a=3.434 c=5.1003
c/a	1.48	1.48	1.48
R _{MT} (Å)	Ni=2.4 S=1.99	Ni=2.44 S=1.99	Ni=2.44 S=1.99
Fermi Energy (eV)	0.6335	0.3696	0.3627
Volume (a. u) ³	351.64	354.164	351.64
Convergence energy (Ry)	-7665.32	-4628.57	-6869.23
Bond Length Å	Ni-Ni=2.55 Ni-S=2.35 S-S=3.23	Ni-Ni=3.43 Ni-S=2.35 S-S=3.23	Ni-Ni=2.55 Ni-S=2.35 S-S=3.43

Table 1.2: Effect of Absorption Coefficient on NiS and different electric fields for NiS in different optical regions

Effect of Field on absorption Coefficient (10 ⁴ /cm)	NiS	NiS _{1.5}	NiS _{-1.5}	NiS _{3eV}	NiS _{-3eV}
I.R. Region(At 1 eV)	47	44	50	43	60
Visible Region (At 2 eV)	54	63	64	68	66
U.V Region (At 4 eV)	27	50	24	14	70

For Ni deficient Ni⁺S, we also observe an optical bandgap (0.5 eV) which confirms the experimental optical bandgap of 0.814 for Ni₂S_{2-x} (Sulphur deficient) [10] thin films. Results for Ni or S deficient bulk NiS are not yet available.

From above description it may be seen the changing behaviour in different region may be due to different contributions of Ni-d and S-p states. On the application of different fields we may do enhancement or reduction in the intensity of transitions in different regions according to our need.

Reflectivity Spectra:

The selected compounds show anisotropic behavior so reflectivity is plotted in xx and zz direction separately. We noticed from the partial density of states (PDOS) of NiS that at Fermi level Nickel-d states and Sulfur-p states have main contribution. When we remove one Ni atom, the number of d-states of Ni atom and Sulfur-p were observed to decrease and when we remove one sulfur atom the Ni-d states and S-p states were observed to increase as a result we see the variation in reflectivity spectra. We also noted that on Ni extraction Ni-d states decreased, so Ni⁺S have highest transmittance.

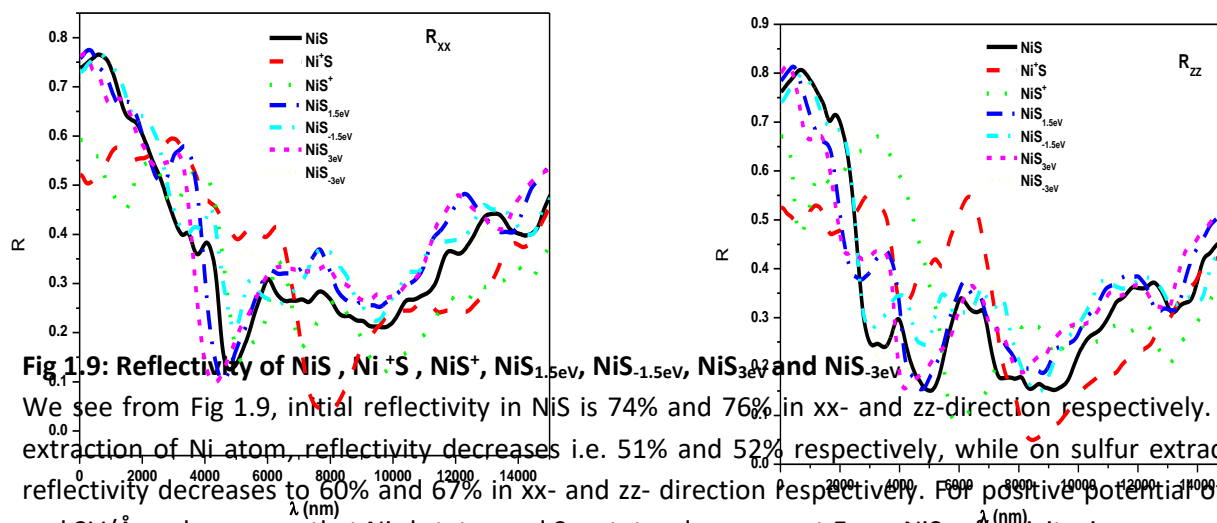


Fig 1.9: Reflectivity of NiS, Ni+S, NiS+, NiS_{1.5eV}, NiS_{-1.5eV}, NiS_{3eV} and NiS_{-3eV}
 We see from Fig 1.9, initial reflectivity in NiS is 74% and 76% in xx- and zz-direction respectively. One extraction of Ni atom, reflectivity decreases i.e. 51% and 52% respectively, while on sulfur extraction reflectivity decreases to 60% and 67% in xx- and zz- direction respectively. For positive potential of 1.5 and 3V/Å we have seen that Ni-d states and S-p states decreases at E_F so NiS reflectivity increases upto 76% and 80% in xx and zz-direction respectively, while for negative potential of -1.5 and -3V/Å, reflectivity decreases i.e. 72 and 75% in xx-and zz-direction.

We compare our results with reflectivity spectra of NiS thin film [12]. At 2500 nm wavelength, reflectivity increases upto 40% only while in our case reflectivity in xx-direction at 2500 nm is 51% and in the zz direction it is 40%. From above discussion, reflectivity in zz direction matches the reflectivity for thin film. In both xx and zz direction Ni+S has highest transmittance.

Refractive Index:

In Fig 1.10, refractive index is plotted for NiS, Ni+S and NiS+ in both xx and zz directions.

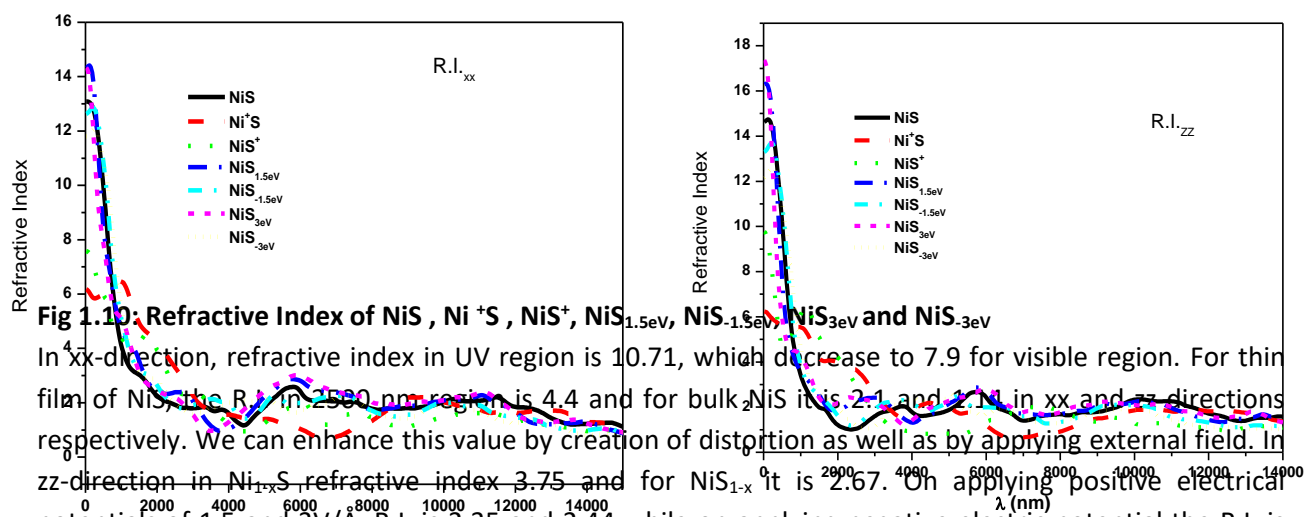


Fig 1.10: Refractive Index of NiS, Ni+S, NiS+, NiS_{1.5eV}, NiS_{-1.5eV}, NiS_{3eV} and NiS_{-3eV}
 In xx-direction, refractive index in UV region is 10.71, which decrease to 7.9 for visible region. For thin film of NiS, the R.I. in 2500 nm region is 4.4 and for bulk NiS it is 2.1 and 1.1 in xx and zz directions respectively. We can enhance this value by creation of distortion as well as by applying external field. In zz-direction in Ni+S, refractive index 3.75 and for NiS_{1-x} it is 2.67. On applying positive electrical potentials of 1.5 and 3V/Å, R.I. is 2.35 and 2.44 while on applying negative electric potential the R.I. is 1.24 and 1.05 respectively.

At a one glance from Fig. 1.10 we observed that in UV region the value of refractive index is very high and is lowered in visible region. On the creation of distortion in NiS, the value of refractive index is 6.39, 5.32 and 2.35 for NiS⁺, Ni+S and NiS respectively i.e. NiS⁺>Ni+S>NiS. In UV region the order of refractive index in xx direction is the order NiS_{1.5eV} > NiS_{3eV} > NiS > NiS_{-1.5eV} > NiS_{-3eV} > NiS⁺ > Ni+S. On applying electrical potentials the order of refractive index is NiS_{+1.5 eV} > NiS_{-1.5 eV} > NiS_{-3 eV} > NiS_{+3 eV} > NiS > Ni+S > NiS⁺, in near IR region Ni+S > NiS⁺ > NiS_{+1.5eV} > NiS_{3eV} > NiS_{-3eV} > NiS and in I.R. region at 7000nm NiS_{3eV} > NiS_{1.5eV} > NiS > NiS.

$1.5\text{eV} > \text{NiS}^+ > \text{NiS}_{-3\text{eV}} > \text{Ni}^+\text{S}$. From above study we see refractive index is different in I.R., U.V. and near I.R. regions. So from above discussion we can conclude that in different region NiS may be used like a sensor.

1.3.4 Transport properties:

Electrical Conductivity and resistivity:

We have plotted electrical resistivity with temperature to see its variation [Fig 1.11].

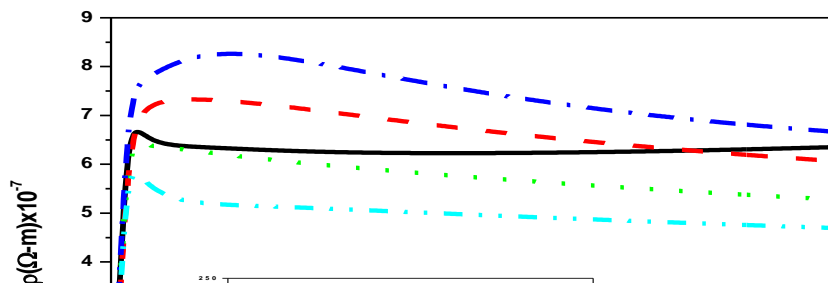


Fig 1.11: Electrical resistivity of NiS, Ni⁺S, NiS⁺, NiS_{1.5V/Å}, NiS_{-1.5V/Å}, NiS_{3V/Å}
 We noted that NiS resistivity is very low. When we change its stoichiometry and on the application of positive and negative potential of 1.5 and 3V/Å, the order of resistivity changes is Ni_{1-x}S > NiS_{1-x} > NiS and NiS_{3eV} > NiS_{1.5eV} > NiS > NiS_{-1.5eV} > NiS_{-3eV}. From the graph we also see that for all different aspects of study Ni_{1-x}S has highest resistivity and NiS at electrical potential of 3V/Å has lowest resistivity. From literature survey, we found the millerite NiS [12] has a high metallic conductivity of $2 \times 10^4 (\Omega\text{-cm})^{-1}$ while hexagonal NiS has a lower value of $1.6 \times 10^4 (\Omega\text{-cm})^{-1}$. Both phases have resistivity of nearly same order, though we may use either hexagonal or millerite phase.

Hall Coefficient:

In fig 1.12 we have seen the variation of Hall Coefficient vs temperature and observed that Pure NiS has highest hall coefficient whereas it is lowered for positive (3V/Å) potential difference.

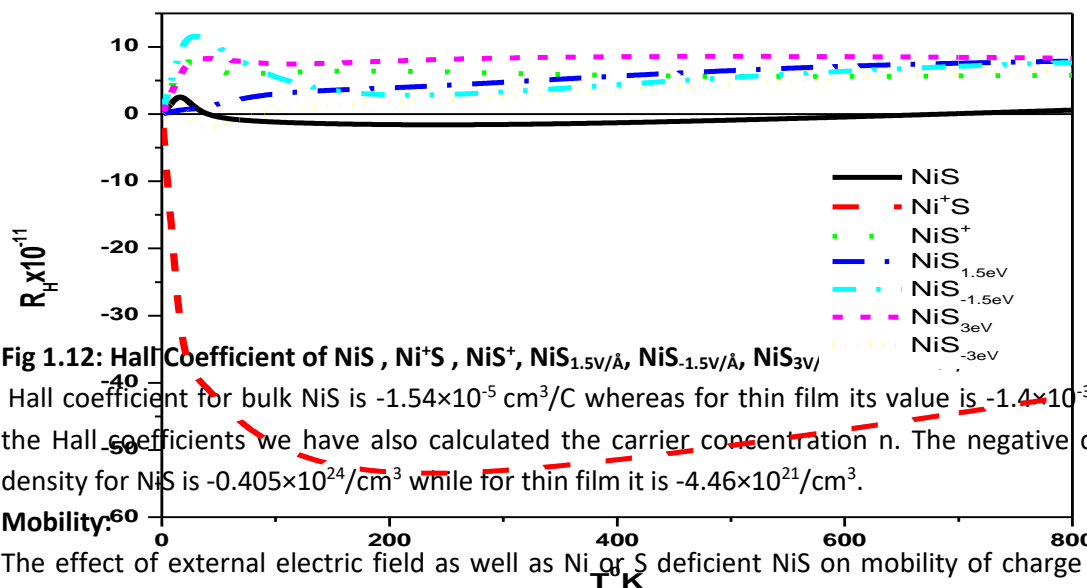


Fig 1.12: Hall Coefficient of NiS, Ni⁺S, NiS⁺, NiS_{1.5V/Å}, NiS_{-1.5V/Å}, NiS_{3V/Å}
 Hall coefficient for bulk NiS is $-1.54 \times 10^{-5} \text{ cm}^3/\text{C}$ whereas for thin film its value is $-1.4 \times 10^{-3} \text{ cm}^3/\text{C}$. From the Hall coefficients we have also calculated the carrier concentration n. The negative charge carrier density for NiS is $-0.405 \times 10^{24} / \text{cm}^3$ while for thin film it is $-4.46 \times 10^{21} / \text{cm}^3$.

Mobility:

The effect of external electric field as well as Ni or S deficient NiS on mobility of charge carriers have been plotted in fig 1.13.

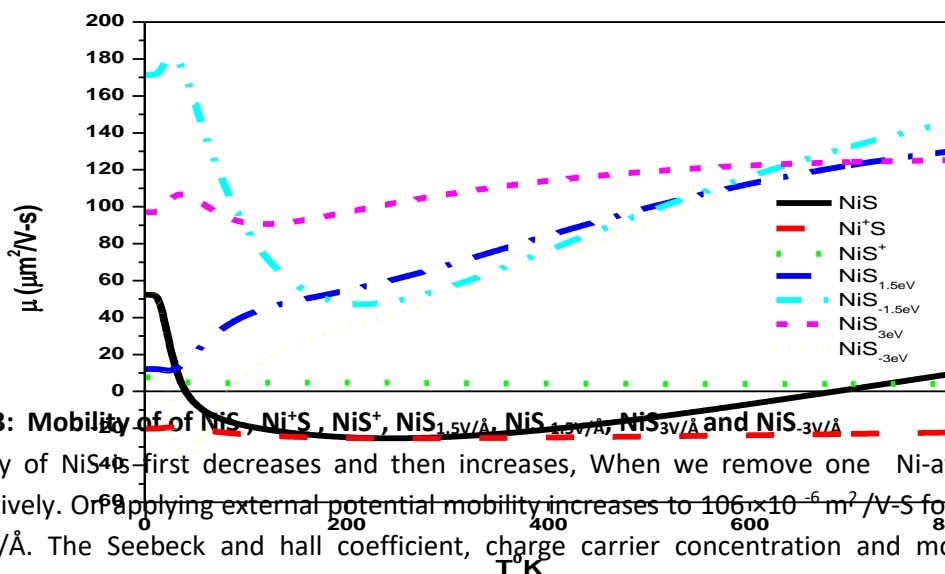


Fig 1.13: Mobility of of NiS, Ni+S, NiS+, NiS_{1.5eV}, NiS_{-1.5eV}, NiS_{3eV} and NiS_{-3eV}
 Mobility of NiS first decreases and then increases, When we remove one Ni-atom and S-atom respectively. Or Applying external potential mobility increases to $106 \times 10^{-6} \text{ m}^2/\text{V-s}$ for the positive bias of $3\text{V}/\text{\AA}$. The Seebeck and hall coefficient, charge carrier concentration and mobility have been tabulated in table 1.3.

Table 1.3: Transport properties of of NiS, Ni +S, NiS+, NiS_{1.5eV}, NiS_{-1.5eV}, NiS_{3eV} and NiS_{-3eV}

Samples/ Properties	NiS	Ni +S	NiS+	NiS _{1.5eV}	NiS _{-1.5eV}	NiS _{3eV}	NiS _{-3eV}
$\sigma(\Omega\text{-m})^{-1} \times 10^6$	1.60	.478	.7458	1.44	1.69	1.27	1.98
$\rho(\mu\Omega\text{-m})$	0.625	2.09	1.34	0.69	0.59	0.78	0.50
$\chi(\text{m}^3/\text{mol}) \times 10^{-9}$	1.21	0.522	1.73	1.35	1.13	1.49	1.12
$n (1/\text{cm}^3) \times 10^{24}$	-0.405	-0.011	.102	0.131	0.189	0.074	0.241
$\mu (\text{m}^2/\text{V-s}) \times 10^{-6}$	-24.6	-253.3	45.3	68.25	55.77	106.0	51.2
C	2.24	0.821	2.98	2.07	1.78	2.47	1.65
K(W/mK)	11.78	3.72	5.24	12.01	13.76	11.05	15.47
S($\mu\text{V}/\text{K}$)	-14.0	-33.3	-.019	-29.1	-32.5	-23.7	-33.4
$R_H(\text{m}^3/\text{C}) \times 10^{-11}$	-1.54	-53.0	6.08	4.74	3.3	8.35	2.59

1.5 Conclusion:

In this work we have studied the hexagonal phase of NiS and compared our results with experiment as well as previous calculated results which are in good agreement. We have performed a comparative

study of Ni-atom and S-atom deficient $Ni_{1-x}S$ and NiS_{1-x} and also studied the effect of applied external potentials. From the above discussions we conclude that millerite and hexagonal NiS phase possess nearly similar characteristics, we may use any one of the phases of NiS. On application of external electric field, NiS shows the possibility of application as optoelectronic material. A deficient of Ni or S leads to increases in transmittance \sim (80%) in IR region.

References:

1. Rajamani, C. T. Prewitt, Canadian Min. **12** 1974 253-257.
2. V. M. Polovov, N. M. Gavrilov, M. P. Kulakov, Sov. Phys. JETP **43** 1976 78-82.
3. E. Barthelemy, C. Chavant, G. Collin and O. Gorochov, J. De Phys. **37** 1976 C4-17- C-4 22
4. D. D. Sarma, S. R. Krishnakumar and N. Chandrasekharan, Phys. Rev. Lett. **80** (1998) 1284.
5. S. R. Krishnakumar, N. Shanthi and D. D. Sharma, Phys. Rev. B **66** 115015-11502 2002.
6. F. Atay, S. Kose, Vildan Bilgin, Idris Akyuz, Turk J. Phys. **27** 2003 285-291.
7. H. Sowa, H. Ahsbahs and W. Schmitz, Phys. Chem. Mine. 2004 321-327.
8. J. Wang, Z. Cheng, J. Bredas and M. Lui, J. Chem. Phys. **127** 2007 214705-214713
9. S. Fan, J. Zhang, C. Xiao, Z. Li, Q. Li, Y. Xie and B. Ye, Solid State Commun. 2014 1-5.
10. A. H. Hammad, Z. S. Elmandouh and H. A. Elmelegi, Acta Physica Polonica-A **127** 2015 901-903.
11. S. K. Panda, P.Thunstrom, DI Marco, J Schott, A Delin, I Dasgupta, O.Eriksson and D D Sarma, New J. Phys. **16** (2014) 093049.
12. R. Boughalmi, R. Rahmani, A. Boukhacham, B. Amrani, K. Driss, Khodja and M. Amlouk, Mata. Chem. Phys. **163** 2015 99-106.